Fibronectin extra domain A stabilises atherosclerotic plaques in apolipoprotein E and in LDL-receptor-deficient mice

Vivek Krishna Pulakazhi Venu[1]; Patrizia Uboldi[1]; Ashish Dhyani[1]; Alessandro Patrini[1]; Roberta Baetta[2]; Nicola Ferri[1,4]; Alberto Corsini[1,4]; Andrés F. Muro[3]; Alberico Luigi Catapano[1,4]; Giuseppe Danilo Norata[1,5]

[1]Department of Pharmacological and Biomolecular Sciences, Università degli Studi di Milano, Milan, Italy; [2]IRCCS Centro Cardiologico Monzino, Milan, Italy; [3]International Center for Genetic Engineering and Biotechnology, Trieste, Italy; [4]IRCCS Multimedica, Milan, Italy; [5]Centro SISA per lo studio dell'Aterosclerosi, Ospedale Bassini, Cinisello Balsamo, Italy

Summary

The primary transcript of fibronectin undergoes alternative splicing in the cassette-type EDA and EDB exons and in the IIICs segment to generate different protein isoforms. Human carotid atherosclerotic plaques with a more stable phenotype are enriched with EDA containing fibronectin (FN-EDA). The aim of this study was to investigate the role of EDA containing fibronectin during atherogenesis. Mice constitutively expressing or lacking the EDA domain of fibronectin ($EDA^{+/+}$ or $EDA^{-/-}$) were crossed with $ApoE^{-/-}$ or $LDL\text{-}R^{-/-}$ mice and fed with a western type diet for 12 weeks. Lack of FN-EDA resulted in reduced atherosclerosis and in a plaque phenotype characterised by decreased calponin positive VSMC's (-15 %) and increased macrophages (+20 %). This was paralleled by increased MMP2, MMP9, and reduced TIMP2, collagen 1A1, 1A2 and 3A1 gene expression compared to that of wild-type and $EDA^{+/+}$ mice. *In vitro*, VSMCs and macrophages isolated from $EDA^{-/-}$ mice showed increased MMPs expression and activity compared to wild-type or $EDA^{+/+}$ mice. Albumin-Cre recombinase/$EDA^{+/+}$/$ApoE^{-/-}$ mice, which produce EDA containing FN only in peripheral tissues, presented an extension, a composition and a gene expression pattern in the atherosclerotic lesions similar to that of controls. The inclusion of EDA in FN results in larger atherosclerotic plaques compared to mice lacking EDA but with a more favourable phenotype in two animals models of atherosclerosis. This effect depends on the EDA-containing fibronectin produced by cells in the vasculature but not in the liver. These observations set the stage for investigating the properties of circulating EDA containing FN in improving plaque stability.

Keywords

Atherosclerosis, extracellular matrix, lipoproteins

Correspondence to:
Alberico Luigi Catapano
Department of Pharmacological and Biomolecular Sciences
Università degli Studi di Milano
Via Balzaretti 9, 20133, Milan, Italy
Tel.: +39 02 50318302, Fax: +39 02 50318386
E-mail: alberico.catapano@unimi.it
or
Giuseppe Danilo Norata
Department of Pharmacological and Biomolecular Sciences
Università degli Studi di Milano
Via Balzaretti 9, 20133, Milan, Italy
Tel.: +39 02 50318313, Fax: +39 02 50318386
E-mail: danilo.norata@unimi.it

Financial support:
AFM is supported by Friuli-Venezia Giulia Regional Grant LR 26/2005; GDN is supported by Fondazione Cariplo (2010–0768), COST action BM0904, Telethon Foundation (GGP13002) and Piano di Sviluppo UNIMI- Linea B 2013. ALC by a grant from SISA Lombardia.

Received: September 22, 2014
Accepted after major revision: February 5, 2015
Epub ahead of print: April 16, 2015

http://dx.doi.org/10.1160/TH14-09-0790
Thromb Haemost 2015; 114: ■■■

Introduction

Fibronectin (FN), is a key component of the vessel extracellular matrix (ECM) and exists in different isoforms resulting from the alternative splicing of a single primary transcript. The inclusion of the extra domain A (EDA or EIIIA) generates FN-EDA which increases during pathological conditions including graft vs host disease (leading to fibrosis in lung, liver and kidney), diabetes, rheumatoid arthritis, cardiac, and hypertension (1–4). In humans, the presence of EDA containing fibronectin in the carotid plaque was associated with a more stable phenotype, characterised by an increased number of vascular smooth muscle cells, more collagen and less lipids (4) while reduced levels of EDA containing fibronectin were associated with an increased prevalence of abdominal aortic aneurysms (5). These data support the relevance of FN during atherogenesis but do not clarify whether the presence of FN-EDA is only a "positive" association or could have a role in improving the plaque phenotype.

A full elucidation of the contribution of the different FN isoforms during atherosclerosis was limited so far by the complex biology of FN and the embryonic lethality of a full FN knock-out (KO) animal model (1) with data reported that are difficult to reconcile. So far, available data were obtained in a single atheroprone ($ApoE^{-/-}$) background, mainly in mice models with fibronectin devoid of EDA. Indeed the deletion of the alternative spliced EDA isoform ($EDA^{-/-}$) which results in the generation of plasma FN (pFN) both systemically and locally, is associated with reduced atherosclerosis in C57Bl/6 mice (6) and in ApoE KO mice (7). As the latter animals continue to produce pFN in the liver, (but do not produce FN-EDA in peripheral tissues), these findings point to an atheroprotective role of FN devoid of EDA produced in peripheral cells. On the contrary, Rowedder et al. showed that the absence of pFN produc-

tion by the liver was associated with reduced atherosclerotic lesions with less SMCs and lack a structured fibrous cap (8).

To clarify the role of the different FN isoforms during atherogenesis, we therefore took advantage of mice which always include ($EDA^{+/+}$) or exclude ($EDA^{-/-}$) EDA in fibronectin and characterised atherosclerotic plaques in two atheroprone backgrounds ($ApoE^{-/-}$ and $LDL\text{-}R^{-/-}$) by feeding $EDA^{-/-}/ApoE^{-/-}$, $EDA^{+/+}/ApoE^{-/-}$, $EDA^{-/-}/LDL\text{-}R^{-/-}$, $EDA^{+/+}/LDL\text{-}R^{-/-}$ and their controls a western type diet for 12 weeks. We also generated an animal model mimicking closer the physiological condition, with the liver, which contributes circulating FN, producing plasma FN devoid of EDA (pFN $EDA^{-/-}$) and with the vessels generating EDA containing FN (Albumin-Cre recombinase/$EDA^{+/+}/ApoE^{-/-}$ transgenic animals).

Materials and methods

Animal models

The generation of mice which constitutively include EDA ($EDA^{+/+}$) or exclude EDA ($EDA^{-/-}$) in fibronectin was described elsewhere (9, 10). To investigate the effects on atherosclerosis, the animals were crossed with Apo $E^{-/-}$ (Jackson Laboratories, Bar Harbor, ME, USA; Strain: B6.129P2-Apoetm1Unc/J) or $LDLR^{-/-}$ (Jackson Laboratories; Strain:B6.129S7-LDLRtm1Her/J) for at least eight generations (11, 12). The following animal models were generated: $EDA^{-/-}/ApoE^{-/-}$; $EDA^{+/+}/ApoE^{-/-}$; $EDA^{-/-}/LDL\text{-}R^{-/-}$ and $EDA^{+/+}/LDL\text{-}R^{-/-}$. An additional triple transgenic animal model with a conditional liver specific production of FN devoid of EDA (thus resulting in circulating levels of FN similar to those present physiologically) but with FN-EDA produced in the peripheral tissues was generated first by crossing Albumin-Cre recombinase with $ApoE^{-/-}$ to obtain Albumin-Cre recombinase/$ApoE^{-/-}$ and later with $EDA^{+/+}/ApoE^{-/-}$ to obtain an Albumin-Cre recombinase/$EDA^{+/+}/ApoE^{-/-}$. Liver-specific deletion of the EDA exon is possible due to the presence of loxP sites flanking the EDA exon(9).

Albumin-Cre recombinase/$ApoE^{-/-}$ were used as control for the latter group. The investigation conforms to the European Commission Directive 2010/63/EU and was approved by the local authorities (Progetto di Ricerca Protocollo 2009/3 and 2012/2). At eight weeks of age, animals were fed *ad libitum* with western type diet (21%fat, 0.15% cholesterol and 19.5% casein, Harlan, Bresso, Italy) for 12 weeks. Mice were sacrificed with sacrificed with an overdose (250 mg/kg body weight) of a 2.5% tribromoethanol solution (Sigma-Aldrich Chemical Co., St. Louis, MO, USA), followed by cervical dislocation. The heart and the arterial tree were perfused with saline solution under physiological pressure. Then the aortas and the hearts were isolated and paraffin embedded (12).

Plasma fibronectin and lipid analysis and quantification of atherosclerosis

Blood samples were collected in EDTA tubes immediately before death by retro-orbital bleeding and plasma was separated by low-speed centrifugation at 4 °C. The measurement of plasma fibronectin levels was performed by ELISA (Abcam 108849, Fibronectin mouse ELISA kit, Abcam, Cambridge UK); plasma was diluted 1:8,000 (in the diluent buffer provided with the kit) and processed according to the manufacturer instruction. The measurement of plasma lipids was performed by standard enzymatic techniques (ABX for Cobas Mira Plus, Montpellier, France) as described (12). Cross sequential sections 5 µm thick were prepared from the aortic root up to 150 µm after the valve leaflets were no longer detectable, sections analysed at this level are indicated as ascending aorta in the manuscript. For the quantification of atherosclerosis, eight serial sections for the aortic root and eight sequential sections of the ascending aorta were stained with hematoxilin-eosin. Images were captured with Axiovert 200 microscope and the atherosclerotic lesion area was quantified by computer image analysis, using Axiovision LE rel 4.4 software by two blinded observer as described (13). The quantification of the collagen content was performed following picro-sirius red staining, images of the aortas were captured with Axiovert 200 microscope (ZEISS, Milan, Italy) under regular and polarised light, then fibrillar collagen, detected by yellow birefringence, was quantified using OPTIMAS Image analysis software (Media cybernetics, Rockville, MD, USA), capable of colour segmentation and automation by programmable macros, by two blinded observer (12). Data are expressed as the percentage of the total atherosclerotic lesion area covered by fibrillar collagen ± standard deviation (SD).

Immunohistochemistry.

The detection of macrophage, smooth muscle cell was performed as described (12, 14). Briefly, rat anti mouse F4/80 (antigen, AbD Serotec, Oxford, UK; dilution 1:100) for macrophages, rabbit monoclonal to calponin (Abcam; dilution 1:100 and 1:500, respectively), rabbit polyclonal to fibronectin (Abcam; dilution 1:200) and rabbit polyclonal to smooth muscle actin, (Abcam; dilution 1:50 and 1:100, respectively) for smooth muscle cells, or non-immune IgG as a control were used (4 °C overnight) followed by incubation with a secondary biotinylated antibody (anti-rabbit IgG or anti-rat IgG, Vector Laboratories, Burlingame, CA, USA; diluted 1:200 in 1% normal goat serum and phosphate-buffered saline [PBS]) 1 hour (h) at room temperature. Immunoreactivity was visualised using avidin-biotin-peroxidase method (Bio-optica, Milano, S. p.A, Italy) with 3,3'-diaminobenzidine substrate (Sigma, Milan, Italy) as the chromogen. Dehydrated sections were observed using Zeiss Axioskop microscope (Zeiss) and analysed with colour video image analysis system linked to the microscope, for the quantification of the immunoreactive area the Image J analysis software, capable of colour deconvolution and segmentation by programmable macros, was used.

Gene expression analysis

Total RNA from whole aorta samples was isolated and cDNA was generated as as described (15) (four animals from each genotype fed the western type diet for 12 weeks were used for this purpose)(15). Three µl of cDNA were amplified by real time PCR with 1× Syber green universal PCR mastermix (BioRad, Segrate, Italy)

as described (15, 16). The primers used have been described previously (12, 15). Each sample was analysed in duplicate using IQTM-cycler (BioRad). Data were normalised for the housekeeping gene GAPDH.

Isolation of vascular smooth muscle cells and peritoneal macrophages

Four- to six-week-old mice were euthanised by cervical dislocation. The mouse was immobilised on a Styrofoam and paws were pinned. The abdomen and thorax were rinsed with 70% ethanol. The dissection of the mouse was performed with sterile scissors and toothed forceps. The internal organs were dissected using a fine scissors enabling a clear view of the aorta from the arch to abdomen. Immediately, the blood was collected and the aorta was flushed twice using 26G needle with cold sterile PBS. The murine aorta was cleaned from peripheral fat and adventitia. The aorta was dissected horizontally and smaller incisions were made longitudinally. The explants were kept in 100 mm plastic pertri dishes with thick base (Euroclone,s.p.a, Pero MI, Italy) and subjected to mild heat fixation for 5–10 seconds. The explants were supplemented with fresh DMEM High glucose (5 ml) containing 20% FBS with 1% L-glutamine, 1% Penicillin and streptomycin. The presence of VSMCs was observed within one week as the explant is removed after three weeks. The plate is supplemented with DMEM High glucose (5 ml) containing 20% FBS with 1% L-glutamine, 1% Penicillin and streptomycin to enable growth. The cells were then trypsinised and plated for subsequent studies. vSMCs were cultured with DMEM high glucose containing 10% FBS, 1% L-glutamine, 1% penicillin and streptomycin and were used up to passage 15. For experiments cell were pre-incubated overnight with DMEM high glucose containing 0.1% FBS, and then experiments were carried out in serum-free DMEM high glucose.

Peritoneal macrophages were isolated from $EDA^{+/+}$ mice, wild-type or $EDA^{-/-}$ as described (17); mice were sacrificed with an overdose (250 mg/kg body weight) of a 2.5% tribromoethanol solution (Sigma-Aldrich Chemical Co.), followed by cervical dislocation.

Western blotting and SDS page zymography

Western blotting analysis was performed as previously described (15), the following primary antibodies were used: beta actin 1:10,000 (Sigma-Aldrich), KLF4 1:1000 (Abcam ab106629), Smemb (Abcam ab83984), Calponin 1:2000 (Abcam ab46794), Myocardin (Abcam ab22073). Briefly, aorta samples were collected in RIPA buffer (Tris 50 mM, NaCl 150 mM, SDS 0.1%, NP40 1%, 1 mM PMSF) and processed with tissue homogeniser. Protein content was measured by Lowry method. The extract form the aorta of two mice from the same group were pooled and loaded in each gel lane. Three independent western blot analysis were performed (i.e. in total six mice for each group were analysed).

The gelatinolytic activity of MMPs was evaluated as described previously (18). Briefly 30 µg of aortic protein extract or up to 20 µl of cellular supernatant corrected for cellular smooth muscle cells or macrophages protein content were loaded on a 7.5% polyacrylamide gel containing 10% SDS and gelatin 1 mg/ml. At the end of run the gel was washed with 2.5% Triton X-100 and then incubate in activation buffer overnight at 37°C. Gelatinase activity was revealed by negative staining with Coomassie brilliant blue R-250. The gelatinolytic activity was calculated by software-assisted analysis; the extension of the digested band in the gel was directly correlated with MMP activity.

Statistics

Results are reported as mean ± standard deviation (SD). Group differences in continuous variables were determined by one way ANOVA with a Bonferroni post-hoc test. Data were analysed using Graphpad Prism 5.0 for Windows and SPSS Statistics 17.0 softwares.

Results

Absence of EDA inclusion in fibronectin results in reduced atherosclerosis.

We first investigated the atherosclerotic lesions extension in mice fed with a western type diet for 12 weeks. For this purpose 16 mice

Table 1: Characterisation of the mouse models used. Body weight, plasma lipid profile and atherosclerotic lesion extension according to the genotype are presented (Mean ±SD is shown. One way ANOVA with a Bonferroni post-hoc test was used. * $p<0.05$ vs $ApoE^{-/-}$; § $p<0.05$ vs $EDA^{+/+}ApoE^{-/-}$. °$p<0.05$ vs $LDL\text{-}R^{-/-}$; # $p<0.05$ vs $EDA^{+/+}LDL\text{-}R^{-/-}$). For each genotype an equal number of male or female mice were used.

	$EDA^{-/-}ApoE^{-/-}$	$ApoE^{-/-}$	$EDA^{+/+}$ $ApoE^{-/-}$	$EDA^{-/-}$ $LDL\text{-}R^{-/-}$	$LDL\text{-}R^{-/-}$	$EDA^{+/+}$ $LDL\text{-}R^{-/-}$	Alb-Cre $ApoE^{-/-}$	Alb-Cre $EDA^{+/+}$ $ApoE^{-/-}$
Number of animals	16	16	16	12	12	12	8	8
Body weight at sacrifice, g	26.4 ± 2.1	30.0 ± 6.5	26.0 ± 4.0	31.0 ± 3.8	28.0 ± 2.7	30.0 ± 1.4	26.5 ± 4.7	25.0 ± 2.5
Weight Gain, g	6.3 ± 1.1	7.4 ± 0.9	6.0 ± 0.5	8.1 ± 1.1	6.5 ± 1.2	7.4 ± 1.2	5.6 ± 1.2	6.3 ± 0.5
Cholesterol, mg/dl	632 ± 31	693 ± 51	666 ± 31	495 ± 70	490 ± 57	570 ± 46	391 ± 66	333 ± 30
Triglycerides mg/dl	200 ± 17	194 ± 15	181 ± 19	280 ± 23	220 ± 32	212 ± 26	135 ± 16	176 ± 32
Aortic Sinus lesion, mm^2	223 ± 74*§	427 ± 127	436 ± 114	174 ± 55°#	432 ± 160	480 ± 213	381 ± 90	375 ± 46
Ascending aorta lesion, mm^2	128 ± 95*§	339 ± 204	336 ± 133	219 ± 81*§	450 ± 190	405 ± 138	348 ± 50	282 ± 48

for each group on ApoE$^{-/-}$ background and 12 mice for each group on LDL-R$^{-/-}$ background were studied. At sacrifice, body weight, weight gain and plasma lipid profile were similar among the different animal groups (►Table 1). Representative images of the aortic sinus and the ascending aorta of EDA$^{-/-}$/ApoE$^{-/-}$; ApoE$^{-/-}$ and EDA$^{+/+}$/ApoE$^{-/-}$ are presented in ►Figure 1A and B. Atherosclerotic lesion area was significantly reduced in the aortic sinus and in the ascending aorta of EDA$^{-/-}$/ApoE$^{-/-}$ compared to ApoE$^{-/-}$ and EDA$^{+/+}$/ApoE$^{-/-}$ (►Table 1, ►Figure 1C and D). This difference was observed in male and in female mice (Suppl. Figure 1, available online at www.thrombosis-online.com). Also EDA$^{-/-}$/LDL-R$^{-/-}$ mice showed significantly smaller atherosclerotic lesions compared to LDL-R$^{-/-}$ and EDA$^{+/+}$/LDL-R$^{-/-}$ mice both in the aortic sinus as well as in the ascendant aorta (►Table 1, ►Figure 1E and F). Again, this was true both for male and for female mice (Suppl. Figure 2, available online at www.thrombosis-online.com). Plasma levels of fibronectin are significantly lower in EDA$^{+/+}$ mice either on ApoE deficient or LDL-R deficient background compared to EDA$^{-/-}$/ApoE$^{-/-}$, EDA$^{-/-}$/LDL-R$^{-/-}$ or ApoE$^{-/-}$ and LDL-R$^{-/-}$, in agreement with previous findings in EDA$^{+/+}$ or EDA$^{-/-}$ mice not on atherogenic background (6) (Suppl. Figure 3, available online at www.thrombosis-online.com). When fibronectin mRNA and protein expression in the aorta were investigated, FN expression was observed in aortic atherosclerotic plaques, as previously shown (6–8). FN levels were similar when EDA$^{-/-}$/ApoE$^{-/-}$, ApoE$^{-/-}$ and EDA$^{+/+}$/ApoE$^{-/-}$ animals were compared. The same was true in

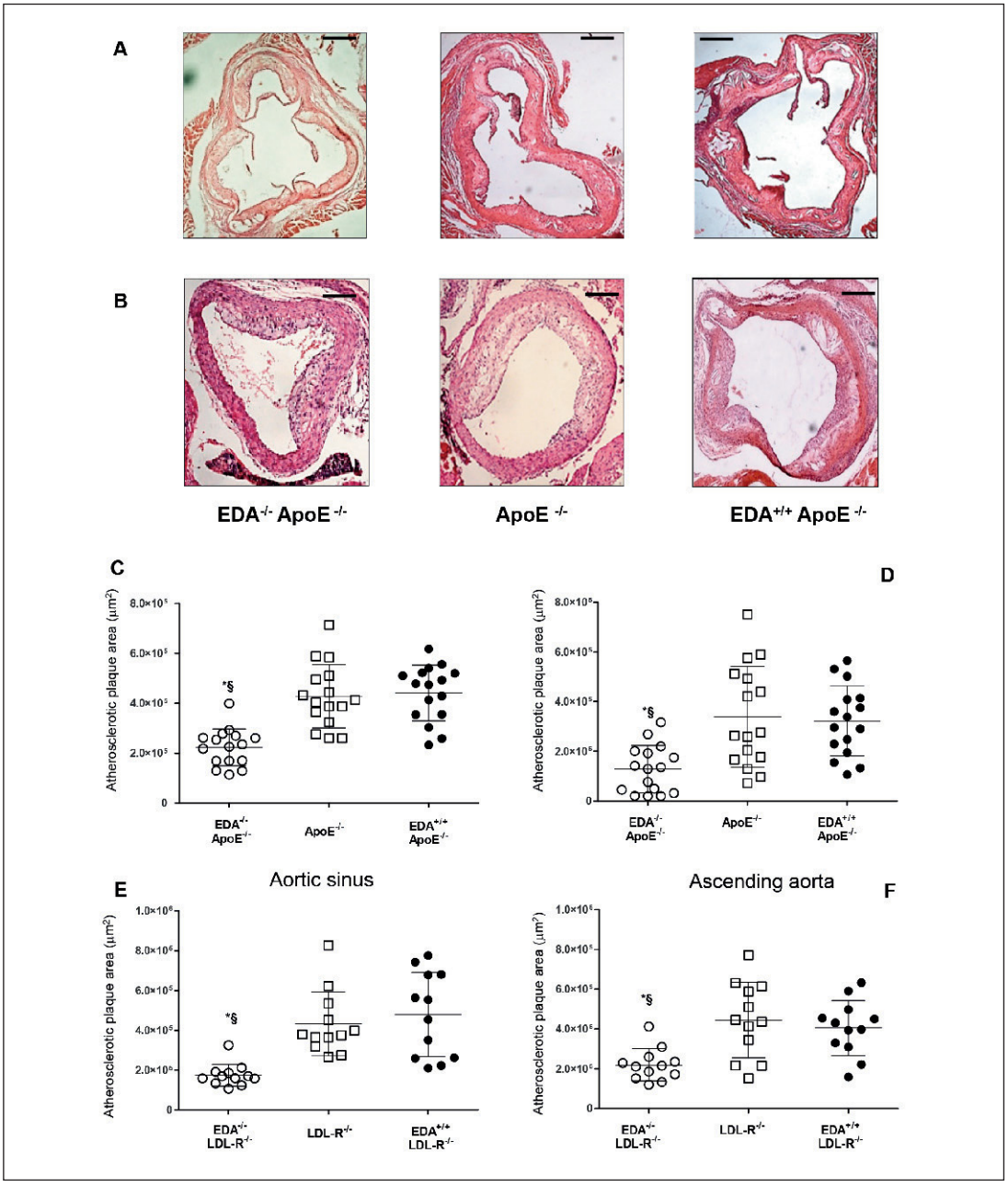

Figure 1: Atherosclerotic lesions in EDA$^{-/-}$ or EDA$^{+/+}$ mice on atherogenic background. A and B) Representative images of the atherosclerotic plaque extension at the level of aortic sinus (A) and ascending aorta (B) in EDA$^{-/-}$/ApoE$^{-/-}$; ApoE$^{-/-}$; and EDA$^{+/+}$/ApoE$^{-/-}$ mice (n=16). C and D) Extension of atherosclerotic plaques at the level of the aortic sinus and of the ascending aorta for EDA$^{-/-}$/ApoE$^{-/-}$; ApoE$^{-/-}$; and EDA$^{+/+}$/ApoE$^{-/-}$ mice. E and F) Extension of atherosclerotic plaques at the level of aortic sinus and ascending aorta for EDA$^{-/-}$/LDL-R$^{-/-}$; LDL-R$^{-/-}$; and EDA$^{+/+}$/LDL-R$^{-/-}$ mice. (Each symbol corresponds to a single mouse; mean ± SD is shown. One way ANOVA with a Bonferroni post-hoc test was used. * $p<0.05$ vs ApoE$^{-/-}$ or LDL-R$^{-/-}$, respectively; $ $p<0.05$ vs EDA$^{+/+}$ApoE$^{-/-}$ or EDA$^{+/+}$ LDL-R$^{-/-}$, respectively. Scale bar =100 µm).

EDA$^{-/-}$/LDL-R$^{-/-}$ mice compared to that of LDL-R$^{-/-}$ and EDA$^{+/+}$/LDL-R$^{-/-}$ (Suppl. Figure 3, available online at www.thrombosis-online.com). Altogether, these data indicate that the absence of EDA in fibronectin is associated with reduced atherosclerotic lesions independently of FN plasma levels and prompted us to investigate whether this difference is also associated with changes in the atherosclerotic plaque composition.

The inclusion of EDA in fibronectin results in increased collagen deposition and calponin expression and decreased MMPs expression and activity in the atherosclerotic plaque.

Next, we characterised collagen deposition in the atherosclerotic plaques of the different animal models. Total collagen levels were significantly decreased in EDA$^{-/-}$/ApoE$^{-/-}$ mice compared to ApoE$^{-/-}$ and EDA$^{+/+}$/ApoE$^{-/-}$ mice, with the latter showing a signifi-

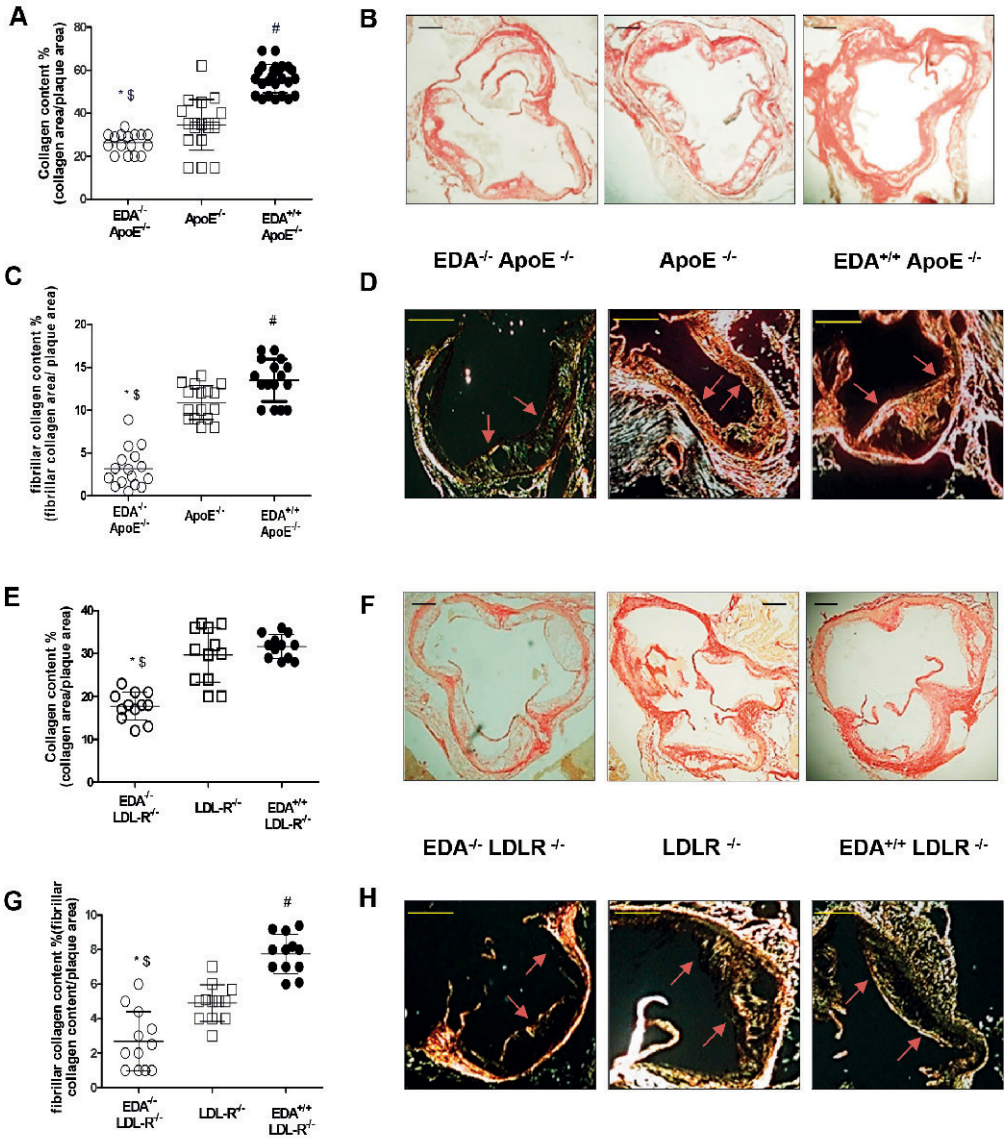

Figure 2: Atherosclerotic plaque collagen content EDA$^{-/-}$ and EDA$^{+/+}$ mice on atherogenic background. A) Collagen content in the atherosclerotic plaque of EDA$^{-/-}$/ApoE$^{-/-}$; ApoE$^{-/-}$; and EDA$^{+/+}$/ApoE$^{-/-}$ mice. Representative images are shown in B. C) Fibrillar collagen content in the atherosclerotic plaque of EDA$^{-/-}$/ApoE$^{-/-}$; ApoE$^{-/-}$; and EDA$^{+/+}$/ApoE$^{-/-}$ mice (n=16). Representative images are shown in D (arrowheads indicate the border with the luminal side). E) Collagen content in the atherosclerotic plaque of EDA$^{-/-}$/LDL-R$^{-/-}$; LDL-R$^{-/-}$; and EDA$^{+/+}$/LDL-R$^{-/-}$ mice. Representative images are shown in F (arrowheads indicate the border with the luminal side). G) Fibrillar collagen content in the atherosclerotic plaque of EDA$^{-/-}$/LDL-R$^{-/-}$; LDL-R$^{-/-}$; and EDA$^{+/+}$/LDL-R$^{-/-}$ mice (n=12). Representative images are shown in H (arrowheads indicate the border with the luminal side). (Symbols are individual mice; mean ± SD is shown. One way ANOVA with a Bonferroni post-hoc test was used. * $p<0.05$ vs ApoE$^{-/-}$ or LDL-R$^{-/-}$, respectively; $ $p<0.05$ vs EDA$^{+/+}$ApoE$^{-/-}$ or EDA$^{+/+}$ LDL-R$^{-/-}$, respectively. Scale bar for panels B and F =100 µm, for panels D and H= 25 µm).

cant increase also vs ApoE$^{-/-}$ mice (▶Figure 2A and B). Further, we characterised the amount of fibrillar collagen contributing to plaque stability by analysing the images under polarised light. An increased amount of fibrillar collagen along the shoulder and around the fibrous cap regions in animals expressing the EDA domain of fibronectin was observed (▶Figure 2C and D). A similar finding for total collagen (▶Figure 2E and F) and for fibrillar collagen (▶Figure 2G and H) was also observed in mice on LDL-R$^{-/-}$

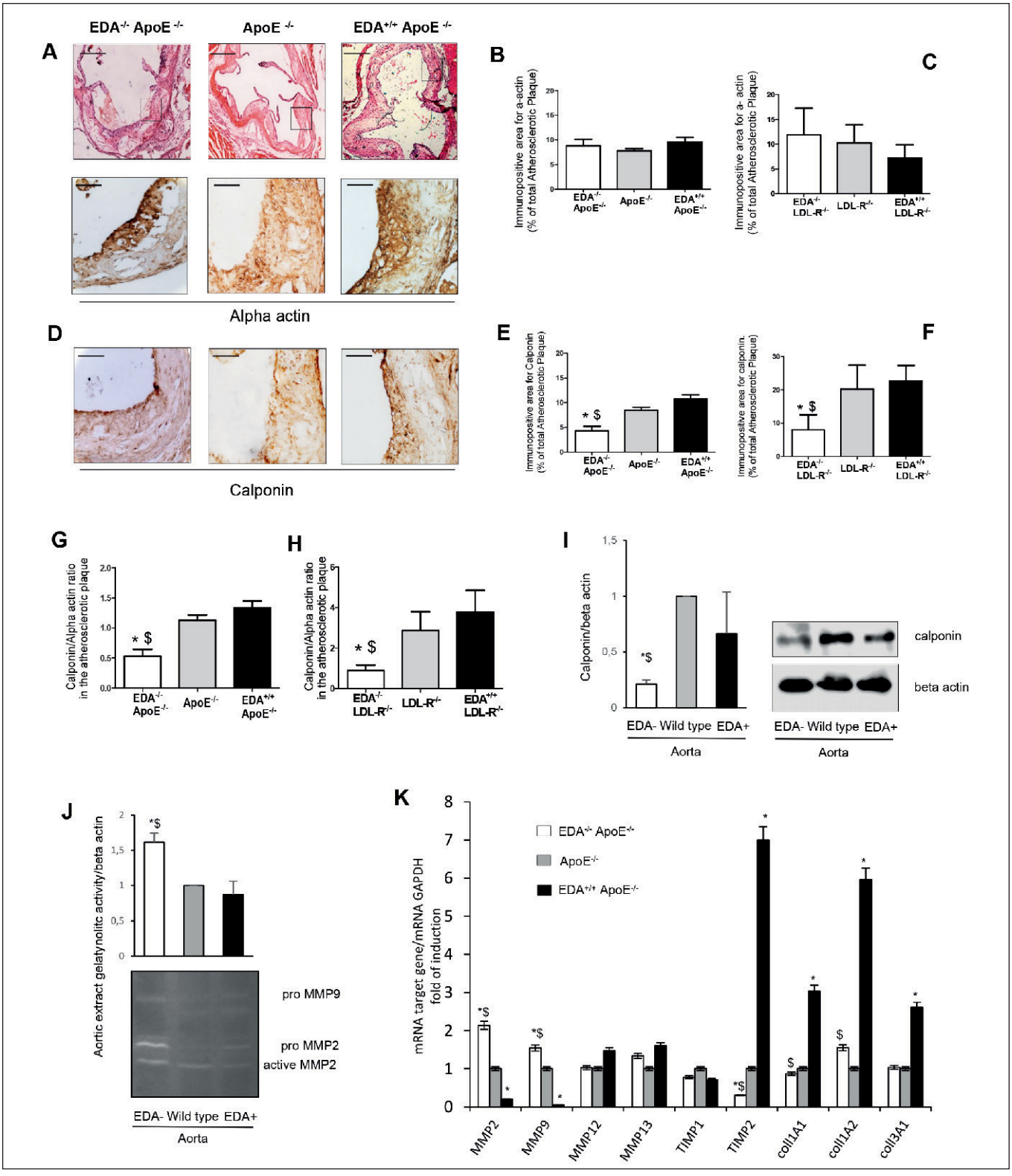

background. These differences prompted us to investigate whether vascular smooth muscle cell distribution and the expression of key genes involved in atherosclerotic plaque remodelling were altered. Although α-smooth muscle actin (SMA) levels were similar in the atherosclerotic plaques of EDA$^{-/-}$/ApoE$^{-/-}$ compared to ApoE$^{-/-}$ and EDA$^{+/+}$/ApoE$^{-/-}$ mice (►Figure 3A and B); those of a specific marker for contractile smooth muscle cell phenotype, calponin (19), were reduced in EDA$^{-/-}$/ApoE$^{-/-}$ compared to ApoE$^{-/-}$ or EDA$^{+/+}$/ApoE$^{-/-}$ mice as detected by immunohistochemistry or western blotting (►Figure 3D, E and I). To confirm that FN with or without EDA could affect the presence of calponin-positive smooth muscle cells in atherosclerotic plaques, a similar characterisation was also performed in mice on LDLR$^{-/-}$ background. In agreement with the findings in mice on ApoE$^{-/-}$ background, α-SMA levels were similar among the three groups (►Figure 3C) while EDA$^{-/-}$/LDLR$^{-/-}$ mice presented reduced levels of calponin (►Figure 3F) compared to LDLR$^{-/-}$ and EDA$^{+/+}$/LDLR$^{-/-}$. Also, the ratio of calponin to α-SMA levels showed a decreased ratio in EDA$^{-/-}$ mice, both on ApoE KO and in LDL-R KO background compared to their controls or to EDA$^{+/+}$/ApoE$^{-/-}$ and EDA$^{+/+}$/LDLR$^{-/-}$ mice (►Figure 3G and H). The same was true when calponin protein levels were measured by western blotting analysis of protein extracts from the aorta (►Figure 3I). To further link the differences in VMSCs phenotype and collagen content with atherosclerotic plaque remodelling we performed gel zymography experiments with protein extracts from the aorta and observed an increased gelatinolic activity in aorta extracts from EDA$^{-/-}$/ApoE$^{-/-}$ mice compared to ApoE$^{-/-}$ and EDA$^{+/+}$/ApoE$^{-/-}$ mice (►Figure 3J). This prompted us to perform a gene expression analysis for matrix metalloproteinases (MMP2, MMP9, MMP12, MMP13, MMP14), for tissue inhibitor of metalloproteinases (TIMP1 and TIMP2) and for collagen 1A1, collagen 1A2 and collagen 3A1 in the aorta of the different mouse models. MMP2 and MMP9 expression was significantly increased in the aorta of EDA$^{-/-}$/ApoE$^{-/-}$ mice while that of TIMP2, was significantly reduced compared to both ApoE$^{-/-}$ and EDA$^{+/+}$/ApoE$^{-/-}$ mice (►Figure 3K). On the contrary EDA$^{+/+}$/ApoE$^{-/-}$ presented significantly increased expression of TIMP2, collagen 1A1, collagen 1A2 and collagen 3A1 mRNA compared to both ApoE$^{-/-}$ and EDA$^{-/-}$/ApoE$^{-/-}$ mice (►Figure 3K). EDA$^{-/-}$/LDLR$^{-/-}$ aorta showed increased MMP2 and reduced collagen 1A1, collagen 1A2 and collagen 3A1 compared to both LDLR$^{-/-}$ and EDA$^{+/+}$/LDLR$^{-/-}$ (Suppl. Figure 4, available online at www.thrombosis-online.com). Furthermore EDA$^{+/+}$/LDLR$^{-/-}$ showed increased expression of collagen 1A1, collagen 1A2 and collagen 3A1 compared to LDLR$^{-/-}$. Overall, both in ApoE$^{-/-}$ and in LDLR$^{-/-}$ mice, the absence of EDA resulted in a gene expression profile compatible with the presence of an atherosclerotic plaque more susceptible to remodelling. Next, we asked whether these differences could be the result of an altered VSMCs function in EDA$^{-/-}$ mice and, therefore, we studied VSMCs isolated from the aorta. We first tested the type of FN produced and showed that wild-type cells produce and release both pFN and FN-EDA+ although the latter to a lower amount compared to VSMCs from EDA$^{+/+}$ mice, while FN-EDA+ production is absent in VSMCs from EDA$^{-/-}$ mice, as expected (►Figure 4A). Collagen mRNA expression was similar in VSMCs from EDA+/+ mice compared to VSMCs from EDA-/- mice and controls (►Figure 4B); therefore, to get further insights into potential effects of FN without the EDA on VMSCs biology, we investigated the presence of key transcription factors associated with vascular smooth muscle cells plasticity such as KLF4 and myocardin. We observed that VSMCs from EDA$^{-/-}$ present an increased expression of KLF4 and a decreased expression of myocardin compared to VSMCs from EDA$^{+/+}$ mice, which points toward a more dedifferentiated and less contractile phenotype in EDA- VSMCs (►Figure 4C and D). This finding was confirmed by the observation that VSMCs from EDA$^{-/-}$ mice have increased Smemb and decreased calponin expression compared to VSMCs from EDA$^{+/+}$ mice (►Figure 4C and D). Furthermore, zymography experiments showed that VSMCs from EDA$^{-/-}$ mice secrete MMPs to a larger extent compared to VSMCs from EDA$^{+/+}$ mice and wild-type mice (►Figure 4E). Gene expression studies further confirmed that VSMCs from EDA$^{-/-}$ mice present a significant increase in mRNA expression not only of MMP2 but also of MMP9, MMP12 and MMP13 compared to VSMCs from EDA$^{+/+}$ or from wild-type mice. Interestingly also TIMP1 mRNA expression was increased (►Figure 4F). We further went on characterising the phenotype of VMSCs and first investigated the migratory response to PDGF to both pFN or EDA+ FN. Both VSMCs from EDA$^{+/+}$ and EDA$^{-/-}$ mice migrated to PDGF and, in agreement with data from Rohwedder et al. (8), cells migrated also toward pFN although to a lower extent to what observed with PDGF (Suppl. Figure 5, available online at www.thrombosis-online.com). The migration of cells toward EDA+ FN was

Figure 3: VMSCs distribution and atherosclerotic plaque gene expression in EDA$^{-/-}$ and EDA$^{+/+}$ mice on atherogenic background. A) Representative images for alpha actin staining in the atherosclerotic plaques of EDA$^{-/-}$/ApoE$^{-/-}$; ApoE$^{-/-}$; and EDA$^{+/+}$/ApoE$^{-/-}$ mice (the areas shown in the lower part of the panel are those indicated by squares in the upper part of the H/E staining) (n=16). B and C) The % of alpha actin immunopositive areas in the atherosclerotic plaques of EDA$^{-/-}$/ApoE$^{-/-}$; ApoE$^{-/-}$; and EDA$^{+/+}$/ApoE$^{-/-}$ mice or of EDA$^{-/-}$/LDL-R$^{-/-}$; LDL-R$^{-/-}$; and EDA$^{+/+}$/LDL-R$^{-/-}$ mice, respectively. D) Representative images for calponin staining in the atherosclerotic plaques of EDA$^{-/-}$/ApoE$^{-/-}$; ApoE$^{-/-}$; and EDA$^{+/+}$/ApoE$^{-/-}$ mice. E and F) Percentage of calponin immunopositive areas in the atherosclerotic plaques of EDA$^{-/-}$/ApoE$^{-/-}$; ApoE$^{-/-}$; and EDA$^{+/+}$/ApoE$^{-/-}$ mice (n=16) or of EDA$^{-/-}$/LDL-R$^{-/-}$; LDL-R$^{-/-}$; and EDA$^{+/+}$/LDL-R$^{-/-}$ mice (n=12), respectively. G and H) Ratio of calponin to alpha actin immunopositive areas in the atherosclerotic plaques of EDA$^{-/-}$/ApoE$^{-/-}$; ApoE$^{-/-}$; and EDA$^{+/+}$/ApoE$^{-/-}$ mice or of EDA$^{-/-}$/LDL-R$^{-/-}$; LDL-R$^{-/-}$; and EDA$^{+/+}$/LDL-R$^{-/-}$ mice, respectively. I) Calponin expression measured by western blotting analysis of four aortas per group and a representative image beta actin and calponin protein content in the aorta of the mice. J) Data for the gelatinolytic activity from three independent experiments for zymography and a representative image. K) Gene expression analysis for genes involved in vascular remodelling in the aorta of the mice (data in panels J and K refer to mice on ApoE KO background) (Mean ±SD is shown. One-way ANOVA with a Bonferroni post-hoc test was used. * $p<0.05$ vs ApoE$^{-/-}$ or LDL-R$^{-/-}$, respectively; $ $p<0.05$ vs EDA$^{+/+}$ApoE$^{-/-}$ or EDA$^{+/+}$ LDL-R$^{-/-}$, respectively. Scale bar panel A, upper part=100 µm, panel A lower part and panel D= 25 µm).

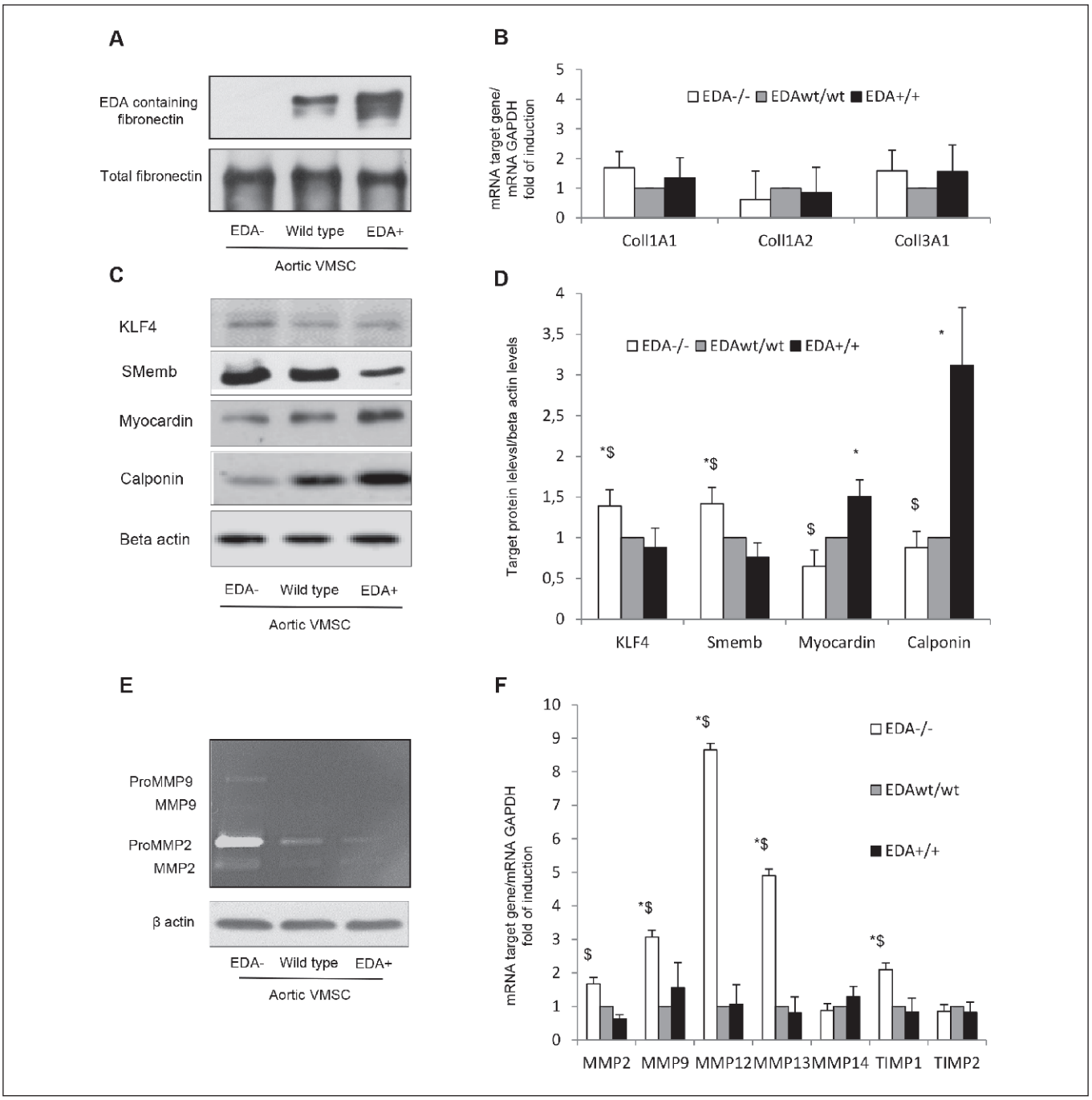

Figure 4: VMSCs properties in EDA$^{-/-}$, wild-type or EDA$^{+/+}$ mice. A) Total fibronectin and EDA containing fibronectin protein in the supernatant of VMSCs isolated from the aorta of EDA$^{-/-}$, wild-type or EDA$^{+/+}$ mice and kept for 24 h in serum free DMEM high glucose. B) Collagen 1A1, 1A2 and 3A1 mRNA expression in VSMCs. C and D) Western blot analysis of KLF4, smemb, myocardin and calponin in VMSCs, a representative panel is presented in C while the analysis of four independent experiments is presented in D. E) Gelatinolytic activity from the supernatant of the cells and correspondent cellular beta actin content. F) Gene expression analysis for genes involved in vascular remodelling in VSMCs (n=6). (Mean ± SD is shown. One-way ANOVA with a Bonferroni post-hoc test was used. * $p<0.05$ vs wild-type; $ $p<0.05$ vs EDA$^{+/+}$, respectively).

similar to that observed with pFN (Suppl. Figure 5, available online at www.thrombosis-online.com).

When the responsiveness of the cells was tested with transforming growth factor, VSMCs from EDA$^{+/+}$ and from wild-type mice showed a similar profile of MMPs induction which was different from that of VSMCs from EDA$^{-/-}$ mice (Suppl. Figure 6, available online at www.thrombosis-online.com) further supporting the existence of different a MMPs expression pattern in VSMCs from EDA$^{-/-}$ mice compared to that of EDA$^{+/+}$ or from wild-type cells under different pathological conditions. As the gene expression

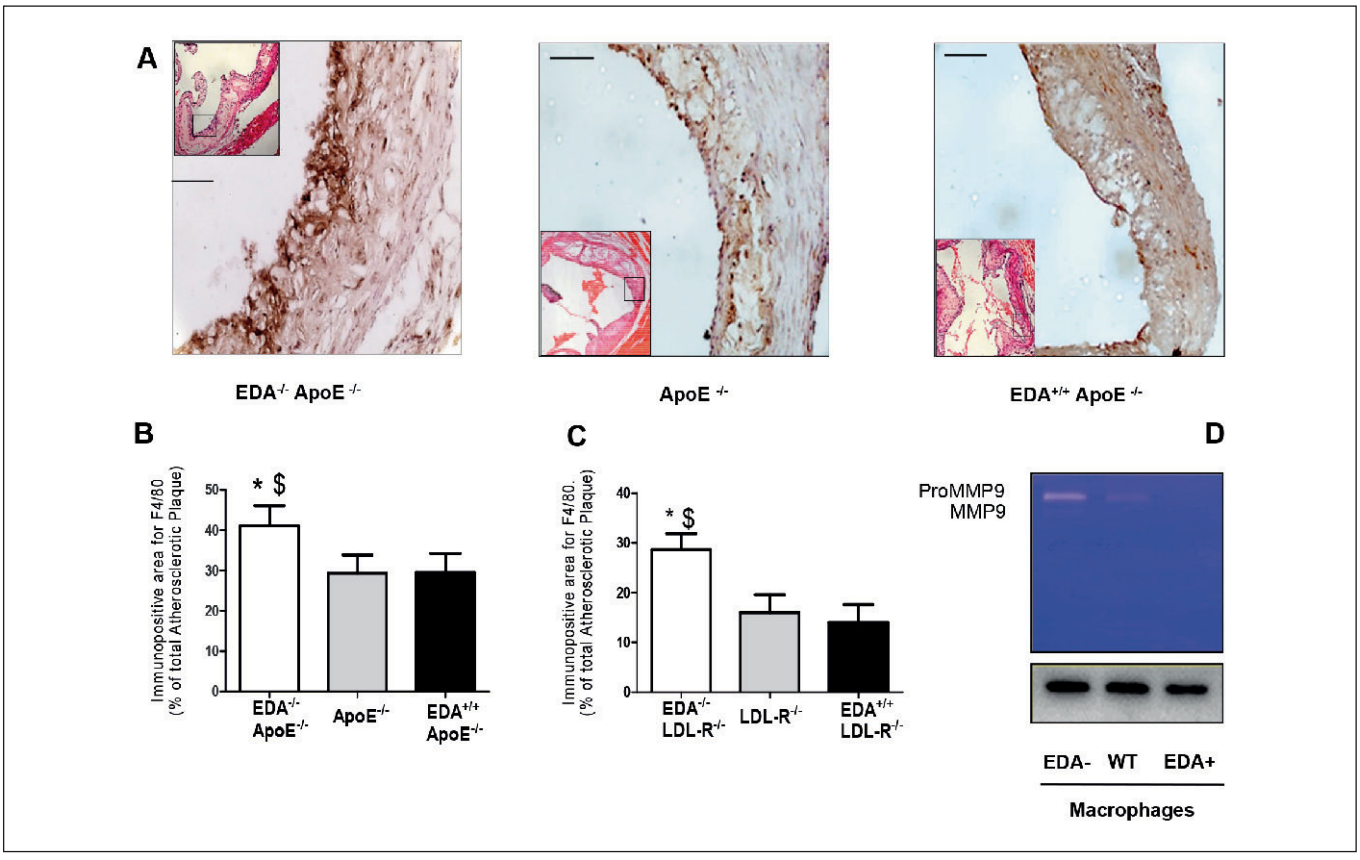

Figure 5: Macrophage content and activity in EDA$^{-/-}$, wild-type or EDA$^{+/+}$ mice. A) Representative images for F4/80 staining in the atherosclerotic plaques of EDA$^{-/-}$/ApoE$^{-/-}$; ApoE$^{-/-}$; and EDA$^{+/+}$/ApoE$^{-/-}$ mice (The H/E staining of the aorta that were selected are presented in the small inside panels). B and C) The % of F4/80 immunopositive areas in the atherosclerotic plaques of EDA$^{-/-}$/ApoE$^{-/-}$; ApoE$^{-/-}$; and EDA$^{+/+}$/ApoE$^{-/-}$ mice (n=16) or of EDA$^{-/-}$/LDL-R$^{-/-}$; LDL-R$^{-/-}$; and EDA$^{+/+}$/LDL-R$^{-/-}$ mice (n=12), respectively. D) Gelatinolytic activity from the supernatant of peritoneal macrophages (n=6). (Mean ± SD is shown. One-way ANOVA with a Bonferroni post-hoc test was used. * $p<0.05$ vs ApoE$^{-/-}$ or LDL-R$^{-/-}$, respectively; $ $p<0.05$ vs EDA$^{+/+}$ApoE$^{-/-}$ or EDA$^{+/+}$ LDL-R$^{-/-}$, respectively. Scale bar = 25 µm).

profile in VMSCs does not completely recapitulate the observations in mouse aortas we asked whether also macrophages expression or activity could be affected in the animal models studied. Macrophages were significantly increased in the aortic lesions of EDA$^{-/-}$/ApoE$^{-/-}$ compared to ApoE$^{-/-}$ and EDA$^{+/+}$/ApoE$^{-/-}$ mice (►Figure 5A and B) and the same was true in mice on LDLR$^{-/-}$ background (►Figure 5C). Gel zymography experiments showed an increased release of MMP9 in the supernatant of macrophages from EDA$^{-/-}$ mice (►Figure 5D). This suggests that both VMSCs and macrophages might contribute to the phenotype observed in the mice.

The absence of EDA in fibronectin produced by cells present in the atherosclerotic lesion contribute to a detrimental atherosclerotic plaque phenotype.

The available findings suggest that while the absence of EDA is associated with a worsened phenotype of atherosclerotic plaques (increased macrophages, increased MMPs, decreased calponin positive VMSCs and decreased collagen mRNA). Contrary to what observed with mice lacking EDA, the inclusion of EDA domain in fibronectin does not affect atherosclerotic plaque extension, but results in plaques with a more favourable phenotype. As under physiological conditions, liver derived fibronectin usually lacks EDA (20), we decided to investigate whether the phenotype observed in EDA$^{-/-}$/ApoE$^{-/-}$ is contributed by circulating liver-derived fibronectin or by FN without EDA locally produced by cells within the atherosclerotic lesions.

To this purpose we generated Albumin-Cre recombinase/EDA$^{+/+}$/ApoE$^{-/-}$ transgenic animals, which mimic EDA$^{-/-}$/ApoE$^{-/-}$ for the production of liver derived (circulating) pFN, which is devoid of EDA, but maintain constitutive inclusion of EDA into FN in the vascular tissues (21). In this animal model, atherosclerosis development was similar to that reported for Albumin-Cre recombinase/ApoE$^{-/-}$ (used as control) (►Figure 6A) as were collagen, α-SMA, calponin and F4/80 positive cells (►Figure 6B-E). Finally gene expression analysis showed a similar profile for MMPs and collagens mRNA in Albumin-Cre recombinase/EDA$^{+/+}$/ApoE$^{-/-}$ mice compared to controls (►Figure 6F). The comparison of the type of fibronectin produced by the Albumin-Cre recombinase/

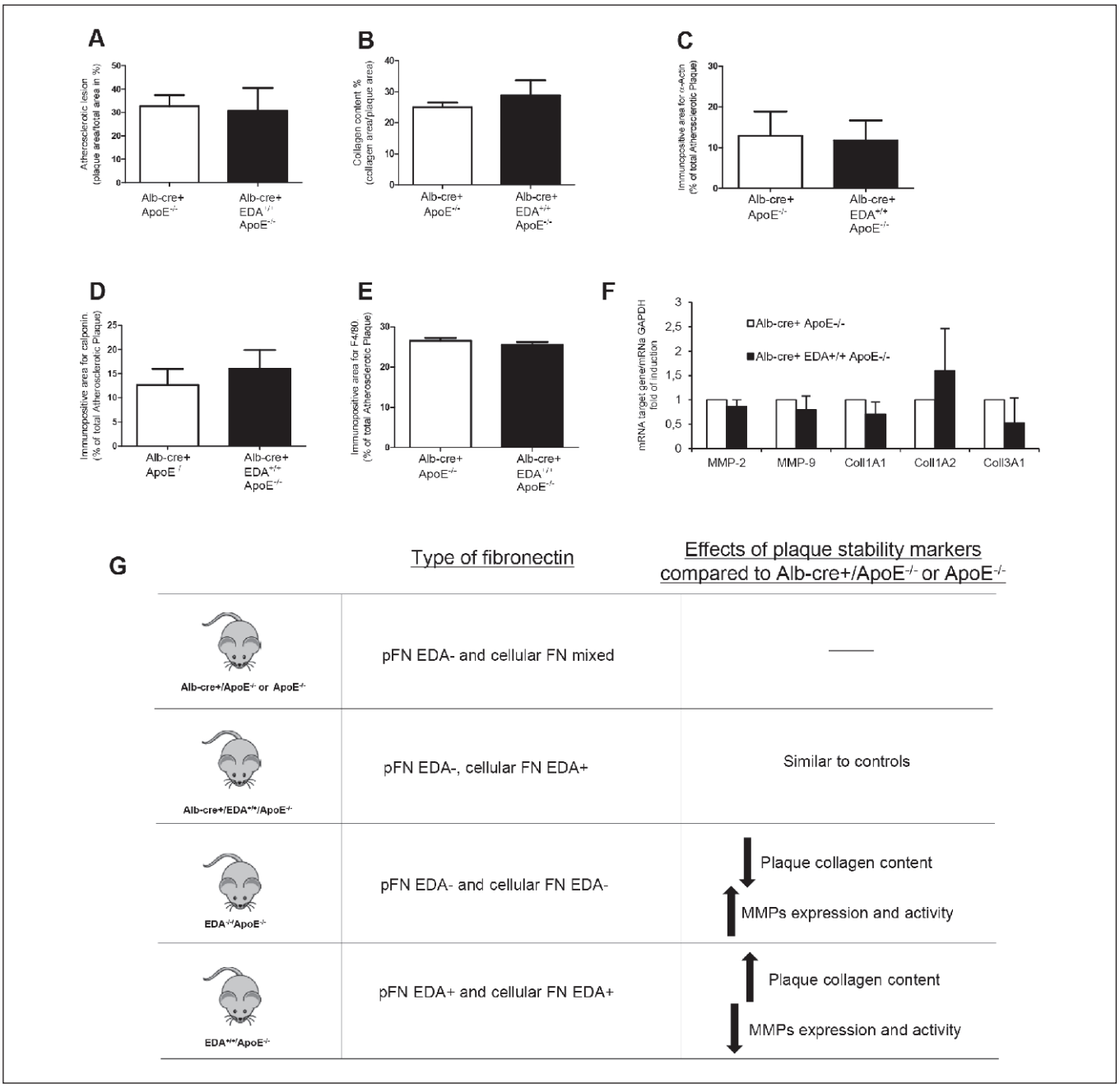

Figure 6: Characterisation of atherosclerotic plaques in alb-cre^{+}/EDA$^{+/+}$/ApoE$^{-/-}$ mice. A) Atherosclerotic plaque development at the level of aortic sinus in alb-cre^{+}/ApoE$^{-/-}$ and alb-cre^{+}/EDA$^{+/+}$/ApoE$^{-/-}$; B-E) Content of total collagen, α-SMA positive vascular smooth muscle cells, calponin positive cells and F4/80-positive cells at the level of aortic sinus in alb-cre^{+}/ApoE$^{-/-}$ and alb-cre^{+}/EDA$^{+/+}$/ApoE$^{-/-}$. F) mRNA levels of matrix metalloproteinases: MMP2, MMP9 and of collagen: coll1A1, coll1A2, and coll3A1 in the aorta of alb-cre^{+}/ApoE$^{-/-}$ and of alb-cre^{+}/EDA$^{+/+}$/ApoE$^{-/-}$ (Mean ± SD is shown (n=8). One way ANOVA with a Bonferroni post hoc test was used. * $p<0.05$ compared to alb-cre^{+}/ApoE$^{-/-}$). G) Schematic picture of the differences in the type of fibronectin, EDA containing (EDA+) or not (EDA-), which is produced in the liver, thus contributing plasma FN (pFN) or locally (cellular FN) in the Alb-Cre/EDA$^{+/+}$/ApoE$^{-/-}$ mice compared to Alb-Cre/ApoE$^{-/-}$ or ApoE$^{-/-}$ used as controls. The differences on plaque stability markers are presented and the comparison with EDA$^{+/+}$/ApoE$^{-/-}$ or EDA$^{-/-}$/ApoE$^{-/-}$ is reported.

EDA$^{+/+}$/ApoE$^{-/-}$ with that of the other animal models (EDA$^{+/+}$ or EDA$^{-/-}$) (▶Figure 6G) clearly suggest that the less favourable plaque phenotype observed in the EDA$^{-/-}$ mice could dependent on the fibronectin lacking EDA which is locally produced by peripheral cells.

Discussion

Our data indicate that, contrary to what observed with mice lacking EDA, the inclusion of EDA domain in fibronectin does not affect atherosclerotic plaque extension, but results in atherosclerotic

plaques with increased collagen expression and with reduced presence of macrophages and MMPs in both ApoE and LDL-R deficient animals.

EDA-FN is prominent in atherosclerotic lesions from mice and humans (7) and we have shown that an important fraction of the FN present in the extracellular matrix is plasma derived (1, 21). Furthermore Rowedder et al. (8) showed in ApoE -/- mice that circulating fibronectin could be deposited at atherosclerotic prone sites. All these observation point to a relevant role of the EDA splice variant under pathological conditions in the cardiovascular system. Structural studies show that the insertion of an extra domain may induce a conformational change that could enhance the potential interaction of FN with surface integrins and other proteins (1). Of note, fibronectin binds collagen and mediates the coassembly of collagen fibrils into the extracellular matrix (22, 23). EDA-FN, which during adulthood is mainly expressed during tissue remodelling, was shown to participate in a correct extracellular matrix assembly (9, 24–26) including the formation of fibrous networks (27). These effects appear to be mediated by the enhancement of the interaction between a5b1-integrin and the nearby cell-binding RGDS sequence, by inducing conformational changes (28). These findings fit with our observation that plaques from EDA+/+/ApoE-/- or from EDA+/+/LDLR-/- display an increased presence of calponin positive cells and fibrillar collagen and support the observation in human carotid arteries, where the levels of EDA-FN were associated with a better plaque phenotype (4).

On the contrary, the lack of the alternatively spliced EDA segment in FN, although associated with reduced atherosclerosis, resulted in an increased presence of macrophages and MMPs, these being clear indicators of an increased inflammatory milieu; as well as reduced collagen expression, supporting the presence of a detrimental plaque phenotype. We also noted a decreased expression of differentiated/contractile markers in $EDA^{-/-}$ VSMCs, a phenotype that has been associated to increased MMPs expression (29, 30), further supporting our findings in $EDA^{-/-}/ApoE^{-/-}$ and $EDA^{-/-}/LDLR^{-/-}$ mice.

We observed that FN plasma levels in $EDA^{+/+}/ApoE^{-/-}$ or $EDA^{+/+}/LDLR^{-/-}$ mice are significantly lower compared to those of $ApoE^{-/-}$ and $LDLR^{-/-}$ and those of $EDA^{-/-}/ApoE^{-/-}$ and $EDA^{-/-}/LDLR^{-/-}$ mice, in agreement with previous findings in mice not on atherogenic background (1, 21). This could suggest that $EDA^{+/+}/ApoE^{-/-}$ or $EDA^{+/+}/LDLR^{-/-}$ could mirror the condition of plasma fibronectin deficiency (8); however, it is unlikely that the effects we observed in the plaque are the consequence of the lower FN circulating levels. Indeed complete plasma fibronectin deficiency was associated with reduced VSMCs and fibrous cap in the atherosclerotic lesions (8). In line with this, our data from the animal model with liver specific deleted EDA production, which present normal pFN levels, suggest that the presence of EDA result in a plaque with a more stable phenotype.

Of note, the animal models used in our study allowed a deep and extensive characterisation of the role of the different FN isoform on atherosclerosis in a setting closer to the physiological condition. Compared to previous observations (6–8), this work includes also a constitutively-expressed fibronectin-EDA ($EDA^{+/+}$) mouse in two atherosclerotic susceptible backgrounds; also Babaev et al. previously investigated the effects of mice which constitutively express fibronectin-EDA, however, this study was performed in 16-month-old C57BL/6J mice not on apolipoprotein E KO background which therefore developed only fatty streaks but not large atherosclerotic plaques. Furthermore, we examined two atherosclerotic regions and provide new information on cellularity and differences in specific matrix proteins. The observation of a different MMPs gene expression pattern and activity *in vitro* in VMSCs and macrophages from $EDA^{-/-}$ mice compared to controls and $EDA^{+/+}$ further point to a negative role of pFN in the tissues.

Overall, our work shows that the presence of FN improves atherosclerosis and more importantly that FN-EDA could contribute to differentiated vascular smooth muscle cell phenotype and to a reduced inflammatory profile in the vasculature and in the plaque. Plasma FN is, however, critical in humans and is needed for a proper response toward bacteria (31). Indeed, low plasma FN levels are associated with a poor prognosis following infection (31), the logical inference, therefore, is that limiting pFN deposition in the atherosclerotic lesions could not be a suitable approach. Data from the liver specific deletion of EDA indicate that the less favourable plaque phenotype observed in the $EDA^{-/-}$ mice could dependent on the absence of EDA-FN locally-produced by peripheral cells and set the stage for further investigating the properties of FN-EDA in improving plaque stability in the context of vulnerable plaques.

What it is known about this topic?

- The exclusion of EDA from fibronectin in generally associated with decreased atherosclerosis although not all literature is consistent in this.

What does this paper add?

- We generated for the first time both mice either lacking or including EDA in fibronectin in two atherogenic backgrounds, apoE KO and LDL-R KO. In both cases the absence of EDA results in reduced atherosclerotic plaques but with a less favourable phenotype.
- EDA inclusion in fibronectin is associated with atherosclerotic plaques with a better phenotype.
- This work sets the stage for further investigating the properties of FN-EDA in improving plaque stability in the context of vulnerable plaques.

Conflicts of interest
None declared.

References

1. White ES, Baralle FE, Muro AF. New insights into form and function of fibronectin splice variants. J Pathol 2008; 216: 1–14.
2. Arslan F, Smeets MB, Riem Vis PW, et al. Lack of fibronectin-EDA promotes survival and prevents adverse remodelling and heart function deterioration after myocardial infarction. Circulation Res 2011; 108: 582–592.

3. Tersteeg C, Roest M, Mak-Nienhuis EM, et al. A fibronectin-fibrinogen-tropoelastin coating reduces smooth muscle cell growth but improves endothelial cell function. J Cell Mol Med 2012; 16: 2117–2126.
4. van Keulen JK, de Kleijn DP, Nijhuis MM, et al. Levels of extra domain A containing fibronectin in human atherosclerotic plaques are associated with a stable plaque phenotype. Atherosclerosis 2007; 195: e83–91.
5. Paloschi V, Kurtovic S, Folkersen L, et al. Impaired splicing of fibronectin is associated with thoracic aortic aneurysm formation in patients with bicuspid aortic valve. Arterioscl Thromb Vasc Biol 2011; 31: 691–697.
6. Babaev VR, Porro F, Linton MF, et al. Absence of regulated splicing of fibronectin EDA exon reduces atherosclerosis in mice. Atherosclerosis 2008; 197: 534–540.
7. Tan MH, Sun Z, Opitz SL, et al. Deletion of the alternatively spliced fibronectin EIIIA domain in mice reduces atherosclerosis. Blood 2004; 104: 11–18.
8. Rohwedder I, Montanez E, Beckmann K, et al. Plasma fibronectin deficiency impedes atherosclerosis progression and fibrous cap formation. EMBO Mol Med 2012; 4: 564–576.
9. Muro AF, Chauhan AK, Gajovic S, et al. Regulated splicing of the fibronectin EDA exon is essential for proper skin wound healing and normal lifespan. J Cell Biol 2003; 162: 149–160.
10. Chauhan AK, Iaconcig A, Baralle FE, et al. Alternative splicing of fibronectin: a mouse model demonstrates the identity of in vitro and in vivo systems and the processing autonomy of regulated exons in adult mice. Gene 2004; 324: 55–63.
11. Ammirati E, Cianflone D, Vecchio V, et al. Effector Memory T cells Are Associated With Atherosclerosis in Humans and Animal Models. J Am Heart Assoc 2012; 1: 27–41.
12. Norata GD, Venu VK, Callegari E, et al. Effect of Tie-2 conditional deletion of BDNF on atherosclerosis in the ApoE null mutant mouse. Biochim Biophys Acta 2012; 1822: 927–935.
13. Tibolla G, Norata GD, Meda C, et al. Increased atherosclerosis and vascular inflammation in APP transgenic mice with apolipoprotein E deficiency. Atherosclerosis 2010; 210: 78–87.
14. Norata GD, Marchesi P, Pulakazhi Venu VK, et al. Deficiency of the long pentraxin PTX3 promotes vascular inflammation and atherosclerosis. Circulation 2009; 120: 699–708.
15. Norata GD, Cattaneo P, Poletti A, et al. The androgen derivative 5alpha-androstane-3beta,17beta-diol inhibits tumor necrosis factor alpha and lipopolysaccharide induced inflammatory response in human endothelial cells and in mice aorta. Atherosclerosis 2010; 212: 100–106.
16. Norata GD, Raselli S, Grigore L, et al. Small dense LDL and VLDL predict common carotid artery IMT and elicit an inflammatory response in peripheral blood mononuclear and endothelial cells. Atherosclerosis 2009; 206: 556–562.
17. Sala F, Aranda JF, Rotllan N, et al. MiR-143/145 deficiency attenuates the progression of atherosclerosis in Ldlr-/-mice. Thromb Haemost 2014; 112: 796–802.
18. Bellosta S, Via D, Canavesi M, et al. HMG-CoA reductase inhibitors reduce MMP-9 secretion by macrophages. Arterioscler Thromb Vasc Biol 1998; 18: 1671–1678.
19. Rensen SS, Doevendans PA, van Eys GJ. Regulation and characteristics of vascular smooth muscle cell phenotypic diversity. Netherl Heart J 2007; 15: 100–108.
20. Tamkun JW, Hynes RO. Plasma fibronectin is synthesized and secreted by hepatocytes. J Biol Chem 1983; 258: 4641–4647.
21. Moretti FA, Chauhan AK, Iaconcig A, et al. A major fraction of fibronectin present in the extracellular matrix of tissues is plasma-derived. J Biol Chem 2007; 282: 28057–28062.
22. Engvall E, Ruoslahti E, Miller EJ. Affinity of fibronectin to collagens of different genetic types and to fibrinogen. J Exp Med 1978; 147: 1584–1595.
23. Gildner CD, Lerner AL, Hocking DC. Fibronectin matrix polymerization increases tensile strength of model tissue. Am J Physiol Heart Circul Physiol 2004; 287: H46–53.
24. Clark RA. Fibronectin in the skin. J Invest Dermatol 1983; 81: 475–479.
25. Jarnagin WR, Rockey DC, Koteliansky VE, et al. Expression of variant fibronectins in wound healing: cellular source and biological activity of the EIIIA segment in rat hepatic fibrogenesis. J Cell Biol 1994; 127: 2037–2048.
26. Serini G, Bochaton-Piallat ML, Ropraz P, et al. The fibronectin domain ED-A is crucial for myofibroblastic phenotype induction by transforming growth factor-beta1. J Cell Biol 1998; 142: 873–881.
27. Abe Y, Bui-Thanh NA, Ballantyne CM, et al. Extra domain A and type III connecting segment of fibronectin in assembly and cleavage. Biochem Biophys Res Commun 2005; 338: 1640–1647.
28. Manabe R, Ohe N, Maeda T, et al. Modulation of cell-adhesive activity of fibronectin by the alternatively spliced EDA segment. J Cell Biol 1997; 139: 295–307.
29. Minami T, Kuwahara K, Nakagawa Y, et al. Reciprocal expression of MRTF-A and myocardin is crucial for pathological vascular remodelling in mice. EMBO J 2012; 31: 4428–4440.
30. Howard EW, Crider BJ, Updike DL, et al. MMP-2 expression by fibroblasts is suppressed by the myofibroblast phenotype. Exp Cell Res 2012; 318: 1542–1553.
31. Hesselvik JF. Plasma fibronectin levels in sepsis: influencing factors. Crit Care Med 1987; 15: 1092–1097.

